The Institute of Space and Astronautical Science
Report No. 604, June 1983

Zero Gravity Experiment of Superfluid Helium

By

Masahide MURAKAMI*, Noriyuki NAKANIWA*, Satio HAYAKAWA**,
Toshio MATSUMOTO**, Hiroshi MURAKAMI**, Kunio NOGUCHI**,
Kiichiro UYAMA*** and Hiroshi NAGANO****

(April 6, 1983)

Summary: Superfluid experiment in the zero gravity state was performed with a cryostat aboard a sounding.rocket S-520. The observation of dynamic behavior of liquid helium (HeII), the verification test of a porous plug phase separator with a controling heater, the investigation of the heat transfer and the breakdown of superfluid thin film, and the noise test of a cooled FET pre-amplifier for IR detectors were performed. The experiment showed that the initial bulk fluid motions rather quickly damped and a stable liquid containment in the cryostat was realized, and that a very good temperature uniformity was attained throughout the vessel because all inside surfaces were covered with bulk HeII or thick adsorbed film. The porous-plug was found to work as good as the prediction in the zero-g state. The adsorbed film became thicker in the reduced gravity state than on the ground, but not so thick as the estimate given by the theory of van der Waals adsorption film. Besides these, this experiment added valuable data to practical applications of cryogenic technology to space.

1. INTRODUCTION

Superfluid experiment in zero gravity is of interest in understanding phenomena otherwise controlled by gravity and of crucial importance for the design and control of superfluid cryogenic systems for a variety of space missions [*1*, *2* and *3*]. An onboard superfluid helium experiment had been performed by the JPL group and provided data of scientific and of engineering value [*4*, *5*, *6* and *7*]. This experiment showed that the bulk motions of HeII were sufficiently well damped to allow the control of their effects on experiments and spacecraft attitude control system, and that the superfluid films maintained the high degree of temperature uniformity found in laboratory superfluid helium cryostats. Also made this an operational demonstration of the usefulness of porous-plugs for liquid-vapor separators. However, it has been pointed out that the results of the film experiment was highly influenced by the aluminum powder matrix for the helium reservoir, that the experimental space for the bulk fluid dynamic behavior was rather small, and that a variation of acceleration was not sufficiently large to test the dynamic response of HeII to acceleration. A larger cryostat would be much thermally stable and produce more realistic data for practical applications of HeII to space. The

* Inistitute of Structural Engineering, University of Tsukuba.
** Dept. of Astrophys., Nagoya University, Nagoya.
*** Toshiba Corporation, Fuchu Works.
**** Institute for Solid State Physics, University of Tokyo.

behavior of saturated thick film should also be investigated in zero gravity. The dynamic response of HeII to a wider range of variations of acceleration was demanded to be investigated under the zero gravity background state. We therefore performed a rocket experiment to further investigate the zero-g behavior of superfluid helium [*8*]. The experiment also aimed at a test of the cryogenic system to be employed in an infrared telescope in space (IRTS) planned by the Japanese infrared astronomy group [*9*]. Problems to be tested and investigated under the zero or reduced gravity condition were defined as follows:

i) Dynamic behavior and stability of superfluid helium responding to varying acceleration and in the zero or reduced gravity state, and the damping of fluid motion thus excited in a tank. Microphonic noise of an infrared detector induced by such fluid motion in a container.

ii) HeII liquid-vapor phase separation by the use of porous-plugs; the steady performance and the method of flow rate control.

iii) Temperature stability and uniformity in the HeII tank.

iv) Superfluid thin film; thermal breakdown and dependence of the thickness on acceleration, and zero-g performance of a superfluid heat pipe.

v) Launching site operation for liquid helium.

Several valuable results were obtained from this experiment, which will be applied to the practical design of the IRTS.

2. Vehicle and Flight Record

The cryostat was launched on board a sounding rocket S-520–3 on Feb. 14th, 1982 from the Kagoshima Space Center. The rocket was equipped with an attitude control system for an ultraviolet telescope aboard the same rocket to make a raster scan of a selected sky region [*10*].

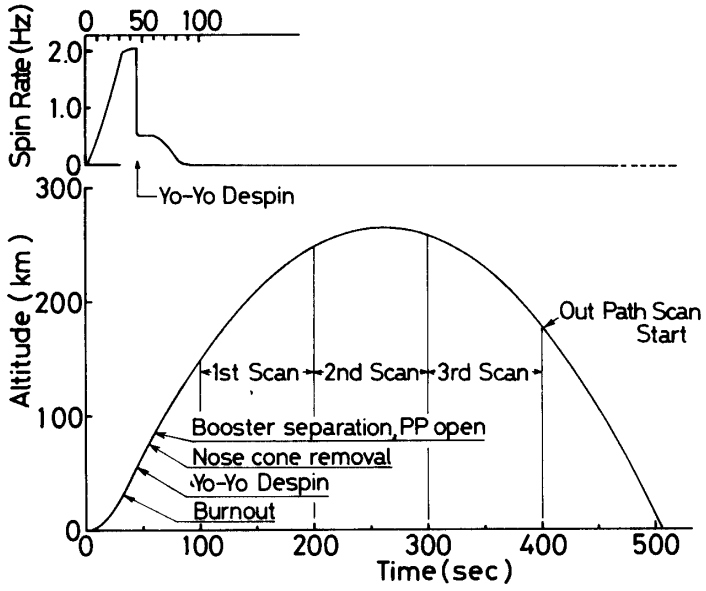

Fig. 1. Altitude and spin rate during flight.

The altitude and the spin rate during the flight as well as operations are shown in Fig. 1. The vehicle started to spin aerodynamically by a small cant of four fins in order to stabilize the attitude. The motor burnout occurred at 32 sec when the spin rate reached 2.1 Hz. Then the yo-yo despin was activated at 46 sec to reduce the rate down to 0.5 Hz. The nose cone was ejected for the UV observation at 55 sec, and the booster was separated from the payload section at 60 sec. The axial component of acceleration reached its maximum 18 g_0, at 26 sec, and then rapidly diminished nearly to zero upon the burnout (g_0 being the gravitational acceleration on the ground). Immediately after the burnout, the rocket suffered a drag force because of the residual atmosphere, and a negative acceleration of -0.35 g_0 was attained at 32 sec. It gradually diminished to zero, and finally the absolute value became basically less than 10^{-3} g_0 except for the acceleration by scan motion. The payload reached an altitude of 263 km at the apogee and splashed down at 504 sec.

The raster scan strated at 101 sec after achieving the zero spin rate and pointing at the first acquisition point. The scan rates were as small as 2 deg/sec for the δ-scan (yawing) for the first three raster scans and about 3 deg/sec for the out path scan started at 402 sec. The acceleration in conjunction with these scan motions was at most 10^{-3} g_0 at the cryostat. More detail will be described later.

The effect of reentry beginning at about 460 sec on the large scale motion of HeII was considerably strong. The payload section set in an autorotation at the final stage of the flight.

3. Cryostat

The cryostat consisted of two SUS cylindrical tanks (4 *l* each), one for HeI as an auxiliary coolant and another for superfluid helium, and of an aluminum vacuum-tight outer shell (330-mm OD, 390-mm high and 45 kg in total mass). The cryostat before the final integration is shown in Fig. 2, in which a supporting stand is also seen. A schematic illustration of the structure is given in Fig. 3-a. A copper cylinder which was soldered to the HeI tank was colled by conduction and worked as the innermost radiation shield at 4 K. It was the primary design point that heat leak to the HeII tank should be anchored to 4 K helium as much as possible. Other two radiation shields which were cooled by helium vapor from the HeI tank surrounded the 4 K shield and the two tanks. In the gaps between the outer shell and two vapor cooled radiation shields were super-insulators (each 20-layers) inserted. Two vacuum-insulated pipes were connected to each thank, one for filling and another for bypassing exhaust line. Beside these lines, exhausting lines for vapor cooling and for a porous-plug phase separator were connected to the HeI and the HeII tanks, respectively, which were not completely shown in the figure. A demountable top plate of the HeII tank was made superleak-tight by In-seal on which four 12-pin-hermetic electrical feedthroughs were mounted.

The HeII tank constituted the experimental space, as schematically illustrated in Fig. 3-a and 3-b: the film flow experiment on the tank axis, 22 superconducting liquid helium II detectors (circles in Fig. 3-a and 1 through 22 in Fig. 3-b), several temperature sensors (T_1 throug T_9), and the porous-plug phase separator (PP in Fig. 3-b). The locations of

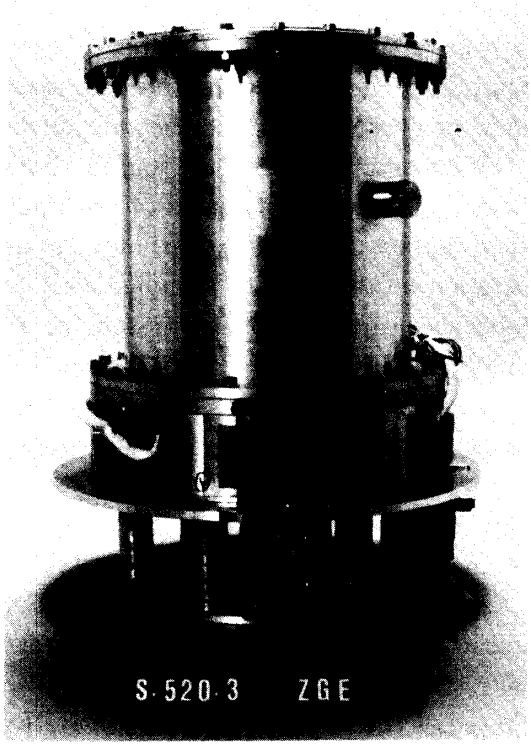

Fig. 2. Experimental cryostat: A vacuum seal-off valve on the main body, five fluid connectors capped plus one valve stem port, and foamed thermal insulator are seen.

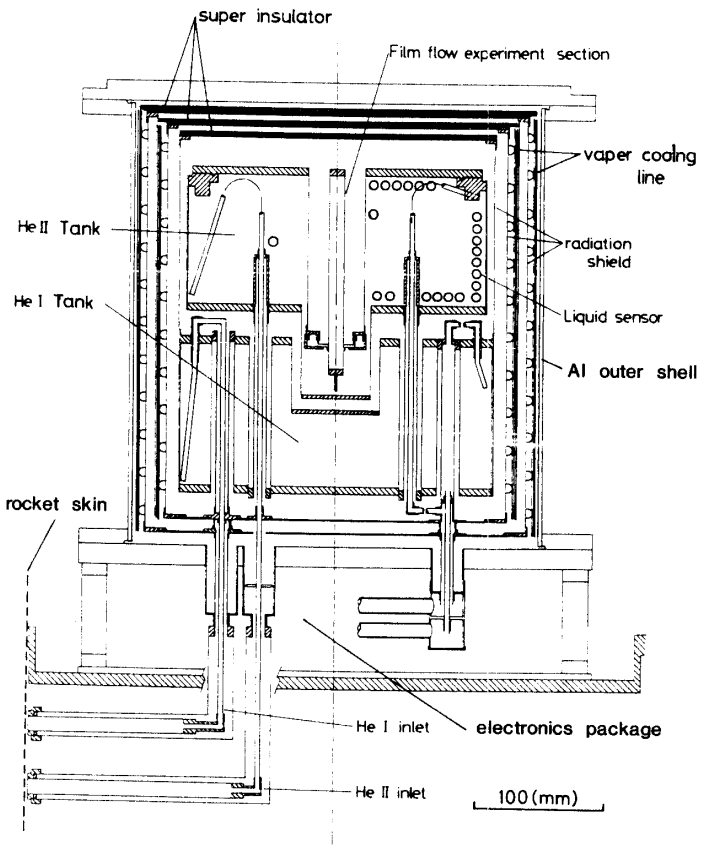

Fig. 3. Experimental cryostat.
a. Structural detail.

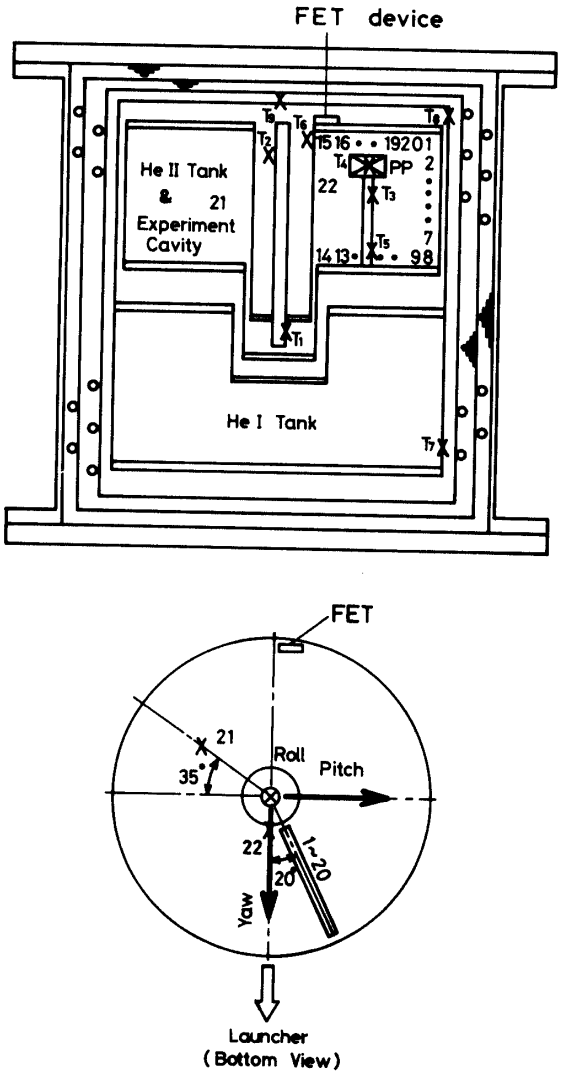

Fig. 3. b. Instrumentation in the HeII tank.

these thermometers are described in Table 1. In addition to these, many copper-constantan thermo-couples were mounted for monitoring temperatures during the ground operation, which were not shown in these figures. The FET device was installed directly on the top plate of the HeII tank. The inside view of the HeII tank is given in Fig. 4, in which the top plate is lifted by hands, and the outer shell is removed. The porous-plug is seen in the lower left of the tank, and an array of liquid detectors, three electrical feedthroughs and the capsule of film flow experiment are also seen on the top plate.

Both axes of the vehicle and the cryostat were carefully aligned with each other. The location of the cryostat was close to the center of mass of the payload section and also to the center of percussion for the attitude control jets. Thus, the effect of scanning motion of the vehicle on the large scale motion of HeII can be minimized during free flight.

The cryogen filling procedure began with precooling of both tanks and filling lines by liquid nitrogen. Subsequently to purging LN_2 and drying the inside, the HeI tank and the HeII tank were filled with liquid helium. In this operation, 10*l* of liquid helium was required for each tank, and slightly less than 4*l* of liquid helium was stored in each tank.

Table 1. Thermometer list

	Location (Function)	Type
T_1	Condensor of Film Flow Exteriment (HeII Temperature)	CRT12
T_2	Evaporater of Film Flow Experiment	GeRT4
T_3	Midpoint in HeII Tank (Monitor for Ground Operation)	CRT24
T_4	Downstream Side of PP	GeRT12
T_5	Lower Point in HeII Tank (HeII Temperature)	CRT11
T_6	Outer wall of HeII tank in Film Flow Experiment Cavity	CRT22
T_7	Outer Wall of HeI Tank (HeI Temperature)	GeRTX
T_8	Upper Point on 4 K Shield	CRT21
T_9	Top Plate of 4 K Shield	CRT23

CRT; Carbon Resistance Thermometer
GeRT; Germanium Resistance Termometer

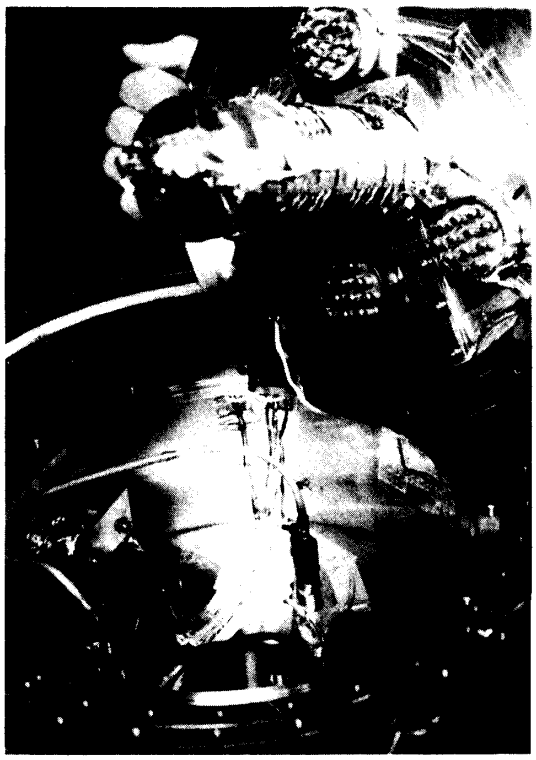

Fig. 4. Inside view of the HeII tank: PP in the lower left, a liquid detector array and three electrical feedthroughs on the top plate, a film flow experiment cavity projecting from it.

The liquid helium in the HeII tank was converted to superfluid liquid helium by pumping, while the liquid in the HeI tank was kept evaporating under the atmospheric pressure condition, and the vapor was exhausted through the vapor cooling line to the environment throughout the experiment. These operations were performed at the launching site 4.5 hr. prior to launch. In the meantime the evacuating pump was kept running except for about one hour for th sake of safety during the operations relating to the main engine and the attitude control system. This fairly long pumping interruption period, in fact, imposed the most serious thermal condition to the cryostat, when heat leak which was not completely absorbed by evaporating HeI resulted in a temperature rise in the HeII tank. Some of the basic design parameters of the cryostat were given by taking this condition into account. The evacuation pump was switched off and the

evacuation line was demounted 3-min prior to launch. The coupling on the rocket skin was closed by a selflocking mechanism upon the demount. The evacuation through the porous-plug began at 60 sec after launch, when the line opened to the outer space mechanically.

4. Experimental Results

(1) Temperature History of the HeI System

The temperature history of the HeI system is given in Fig. 5. Before the launch, the temperature of HeI itself (T_7) was 4.3 K and the 4 K radiation shield (T_9) was at most 16 K at the center of the top plate. This was nearly the expected thermal condition. The temperature of HeI, T_7 gradually dropped subsequent to the launch according to reduction in the vapor pressure, though the reduction was not so fast as that in the atmospheric pressure as the altitude increases. It is quite plausible, judging from the

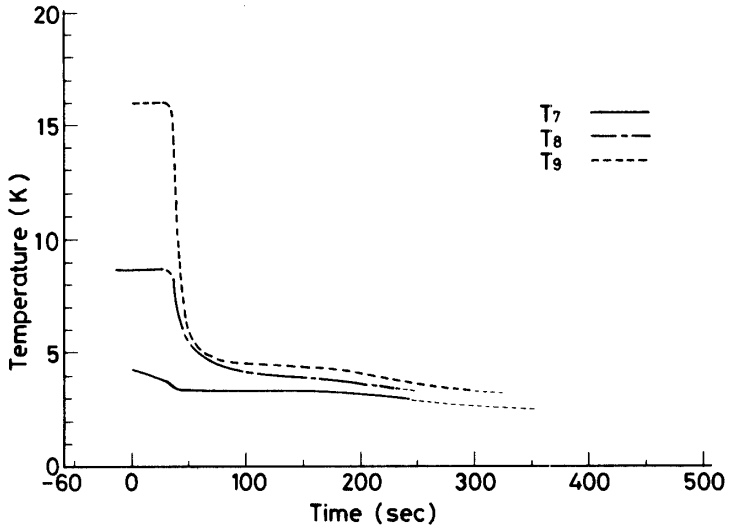

Fig. 5. Temperature history in HeI system.

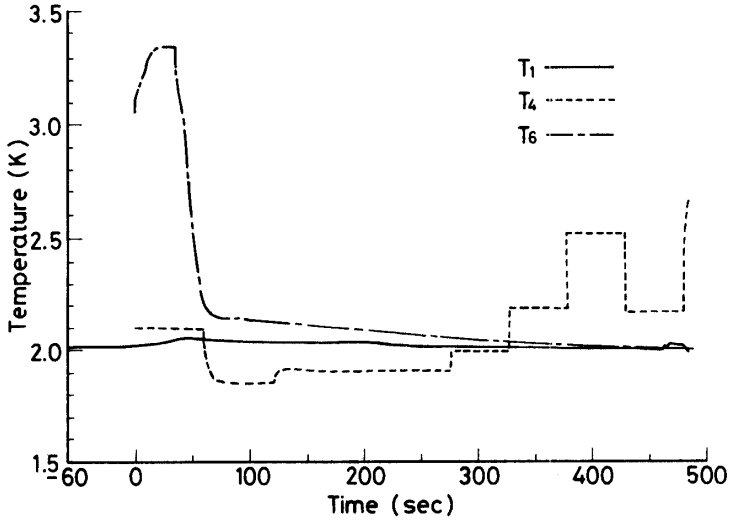

Fig. 6. Temperature history in HeII system.

variations of T_8 and T_9, that some amount of HeI flooded into the vapor exhaust line upon the occurrence of reversal of the fluid position in the tank caused by negative acceleration beginning at 32 sec. However, major part of HeI remained in the tank owing to the correct design of the location of the vapor entrance to the cooling line and owing to a large fluid impedance of the long vapor cooling line, so that only a limited amount flooded out. The flooded liquid helium fully evaporated by 180 sec, then evaporation from the tank resumed, and the temperature again began to drop. It can now be confirmed that a considerably large amount of HeI was left in the tank even at the end of the flight. All the temperatures never rose above 4 K, though the output signal from the thermometers reached the saturation level of the signal conditioners. The heat load to the tank calculated from the evaporation rate just before the launch was about 200 mW, which was fairly close to the design value.

(2) Temperature History of HeII System

The temperature variation is shown in Fig. 6 for the HeII system. The temperature of HeII itself is given by T_1 as it has been confirmed that this represented the temperature of bulk HeII though the thermometer was installed in the condenser section of the film flow experiment. This thermometer was wrapped in a woven copper mesh to maintain direct contact with HeII owing to the capillary effect. The heat leak into the tank was verified to be less than 30 mW just before the launch, when the temperature still went down very slowly. Thus, 50 mW including heat generation by liquid detectors and the film experiment was supposed to be net heat load to the tank during the flight experiment, which was within the design value.

The vapor evacuation line had been closed 3 min. prior to launch, and thus a very slow temperature rise was seen. HeII temperature at the instance of launch was 2.02 K. T_4 indicated a little higher temperature 2.10 K, as the porous-plug was about 3 cm above the liquid surface, and T_6 was 3.05 K, which was the temperature on the outer surface of the upper portion of the HeII tank made of SUS. Subsequently to the launch, a very large acceleration forced the superfluid film covering the inside walls of the tank to thin or to disappear partially and resulted in a rapid rise in T_6. The effect of negative acceleration appeared from 32 sec. Bulk HeII migrated toward the top plate. This gave rise to a slight rise in T_1 by at most 10 mK, because HeII came in contact with the unwetted higher temperature portion of the tank wall, and to a rapid drop in T_6 down to almost HeII temperature. After this period, nearly a zero-gravity situation was realized, and HeII covered more or less uniformly the whole surface in the tank. The tank gradually got to be isothermal. Such development of the liquid situation was also seen from the record of liquid detectors as described later.

Vapor evacuation through the porous-plug was resumed at 60 sec. Immediately after the resumption, liquid helium stayed in the downstream cavity of PP firstly evaporated and T_4 rapidly dropped. Such a situation ended by 120 sec, and effective evacuation from the tank started. All the tempeartures began to drop slowly. The maximum flow rate through this particular porous-plug was adjusted to be about 70 mW according to the preflight test data in this tempearture range, and thus it did not bring about a rapid temperature drop. An experiment to test a method of controlling the flow rate through

the porous-plug was initiated from 277 sec by applying heat to the downstream side of PP. The temperature T_4, thus, changed stepwise. This experiment will be described in the next section.

The temperature of HeII was very stable and that an isothermal state was realized in the tank, though the dynamic behavior of HeII responding to varying acceleration was detected during the flight, and a small amount of heat generated from the experiments was periodically imposed. Thus, all the experiments could be conducted under a constant and uniform temperature condition.

(3) Porous-Plug Phase Separator

A phase separator is of crucial importance for the efficient containment of HeII in a tank in the zero-gravity state. HeII may otherwise easily escape from a tank into venting lines in low- or zero-gravity, as the phase boundary surface can not be well defined in tanks under such conditions. The porous-plug thus plays a role of separating the gas phase from the liquid phase to vent out the former. The thermofluid dynamics of the phase separation in porous-plugs may be treated on the basis of the two-fluid model of superfluid [*10*]. The mechanism of phase separation is based on a thermomechanical effect acting across the porous-plug. The effect makes the superfluid component flow toward the upstream side where the temperature is higher than in the downstream side cooled by evaporating helium. The detail theory and experimental results will be published elsewhere [*11*]. A study of the porous-plug with several materials was presented in the report 12.

The onboard porous-plug was made of ceramic alumina of 2-μm mean pore size. The structure of the porous-plug phase separator is shown in Fig. 7. The size is 22 mm in diameter and 10 mm in thickness. A copper disk pierced with holes for the vapor flow was directly contacted with the downstream side, into which a germanium thermometer and a heater winding were fitted. The PP mount was installed in the HeII tank, so that the opening might be above the liquid surface to prevent liquid from leakage in the period

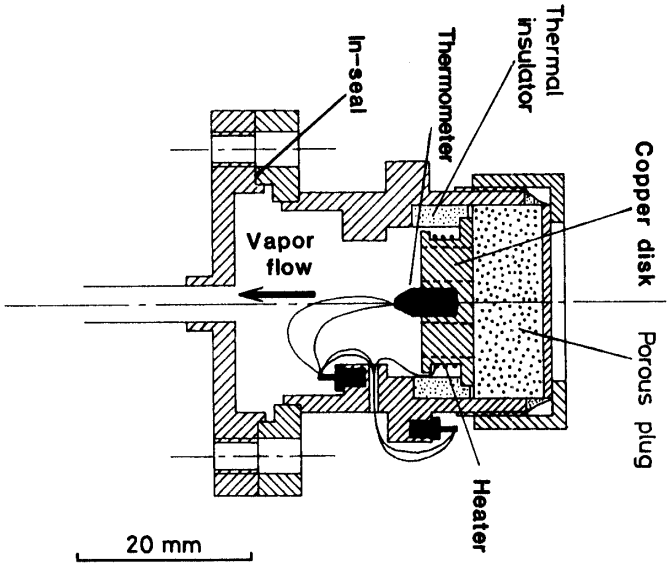

Fig. 7. Structure of porous-plug phase separator.

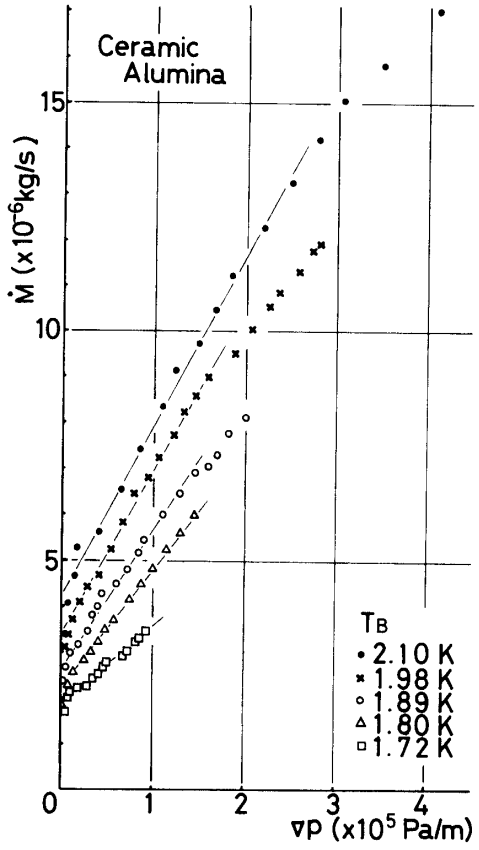

Fig. 8. Flow rate across a porous-plug. (ϕ22 $\times$10 mm thick, mean particle size; 2 μm).

of vacuation interruption prior to launch. Typical flow rate data of a similar PP are given in Fig. 8, in which the mass flow rate $\dot{M}$ is plotted against the pressure gradient ∇p across PP with the HeII temperature (upstream) T_B as a parameter.

As described before, the PP worked stably after 120 sec. An attempt to test the flow control started at 277 sec. The PP produces reversal flow only of the superfluid component. Some amount of heat applied to the downstream side would reduce the temperature difference across the PP to weaken the thermomechnical effect. The effect is the motive force of the reversal flow of the superfluid component, and thus the net flow rate would increase. This has been successfully accomplished in ground tests (see [*11*]). In the flight test, three levels of heating conditions were imposed in four successive periods of 50 sec each; 5 mW from 277 sec, 16 mW from 327 sec and again from 427 sec, 33 mW from 377 sec and from 470 sec. Unfortunately, the flow measurement device was found to malfunction during rocket ascending. However, it may be fair to judge from the record of T_4 that expected functions were performed for the first four heating conditions. In ground tests in which the PP was located above the liquid surface, a dryout in the downstream side always occurred even for the second heating rate, 16 mW, to result in a significant reduction of the flow rate and a temperature jump up far above the lambda temperature, 2.172 K. However, there was no indication of the dryout in the flight data in the first four periods. The upstream side of the PP might be, at least, covered by thick superfluid film under zero-g situation, though it is unceratin whether it directly contacted with bulk HeII or not. This situation is favorable in the application of

this scheme to the flow rate control. In the fifth heating period which started at 477 sec, the PP dryout was certainly observed. A large acceleration caused in conjunction with reentry seems to have diminished the film thickness in the upstream side.

The temperature of HeII T_1 monotonously dropped and the PP downstream side temperature T_4 was always below T_1 except for the periods of a higher heating rate during the flight experiment, though some additional heat from the experiments was periodically added to HeII as a heat sink. These facts may indicate that the porous-plug satisfactorily performed the phase separation throughout the flight experiment.

(4) Dynamic Behavior of HeII

It is one of the primary purposes to see the dynamic behavior of HeII responding to varying acceleration during the flight. This was investigated by the use of three arrays of superconducting liquid HeII dtectors distributed in the tank (Fig. 3-a and b, also Fig. 4), one on the side wall (1 through 8), others on the bottom (9 though 14) and on the top plate (15 through 20), and two single elements (21 and 22). A schematic illustration of an element is given in Fig. 9. This is a kind of hot-wire type detector which consisted of 25-μm-dia manganin wire partly coated with InSn (50–50%), which is quite similar to those used in the JPL rocket experiment [*4*, *5* and *13*]. A constant current of 15 mA was always supplied to all detectors to heat them by Joule heating in the uncoated portion. In vapor, the wire is at a temperature higher than the superconducting transition temperature, about 3 K, because of the low cooling capability of vapor. Thus, the detector indicates higher (normal) resistance. While in HeII, it is enough cooled to be in the superconducting state, and is of lower resistance. This is the principle of distinguishing

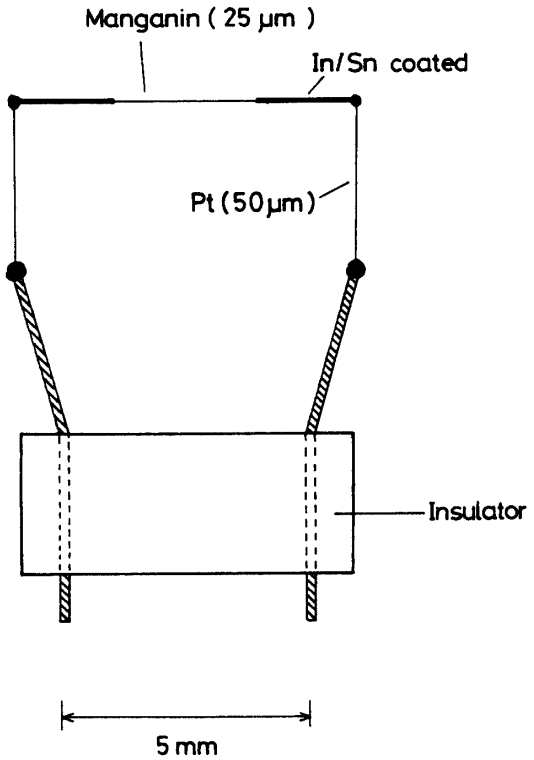

Fig. 9. Superconducting liquid HeII detector.

between liquid HeII and vapor phases. A typical static performance is shown in Fig. 10. The response time was fairly fast, less than 0.1 sec.

Results are presented in Fig. 11-a for the first 65 sec, in Fig. 11-b for the zero-g situation, and in Fig. 11-c for the last stage of the flight, in which black circles and thick lines indicate the immersion in liquid. On the launcher the liquid surface inclined by 12.5 deg from the bottom surface of the tank. From Fig. 11-a, it is easy to see the gradual movement of the HeII surface becoming parallel to the bottom plane because of large axial acceleration, the reversal of the liquid location in the tank during the negative aceleration period starting at 32 se, and then the transition to the spin-dominant state from about 37 sec. Effects of the despin motion around 46 sec, and of the transition motion to the first acquisition point for the raster scan from 62 sec through 70 sec as seen in Fig. 12-a, are also recognized here. Nearly periodical motions which are not precisely shown in Fig. 11-a were detected by two sensors, 10 and 11, which were found from Fig. 11-a to be located near the contact line of the bulk HeII to the bottom. The frequen-

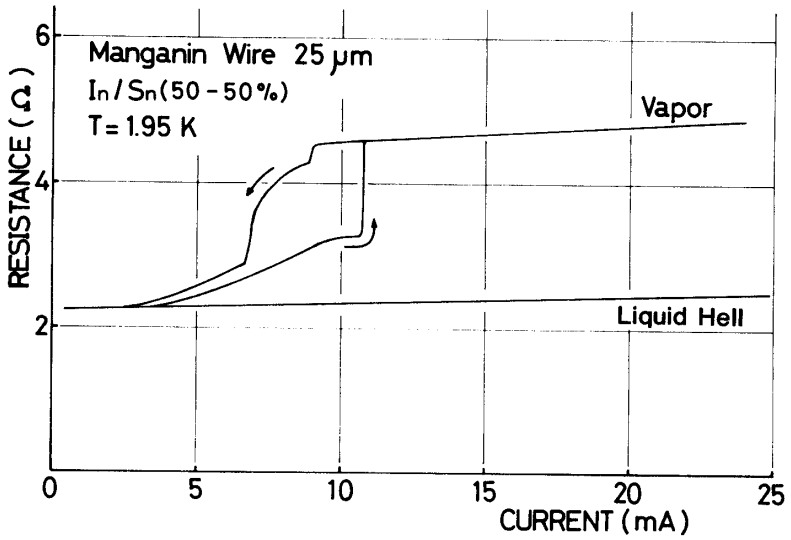

Fig. 10. Static performance of a superconducting liquid HeII detector.

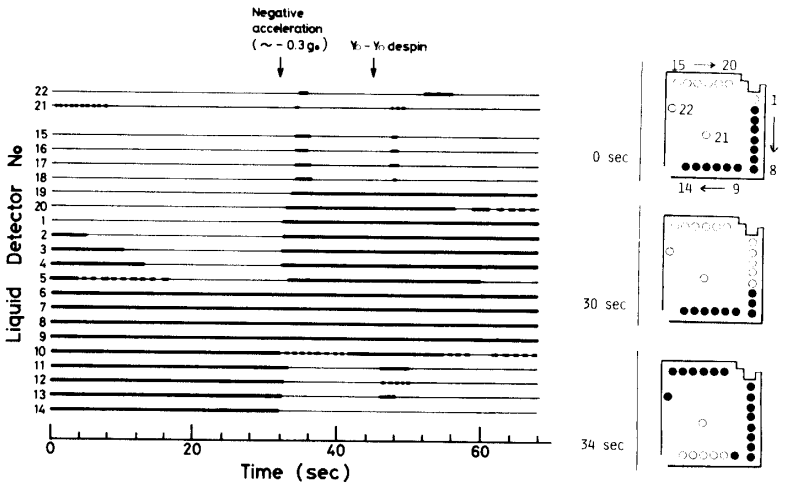

Fig. 11. a.

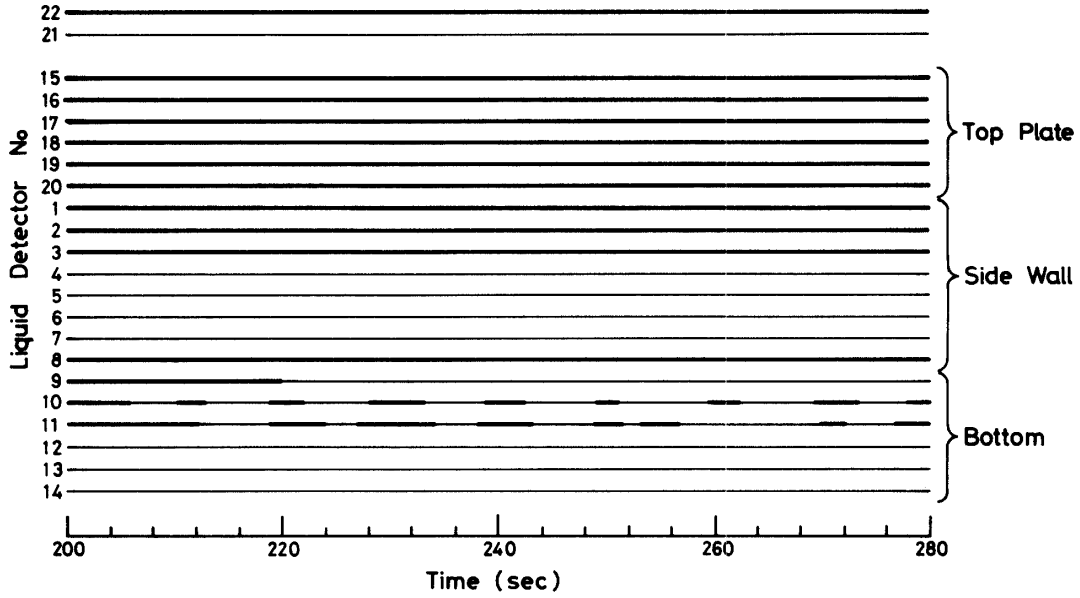

Fig. 11. b.

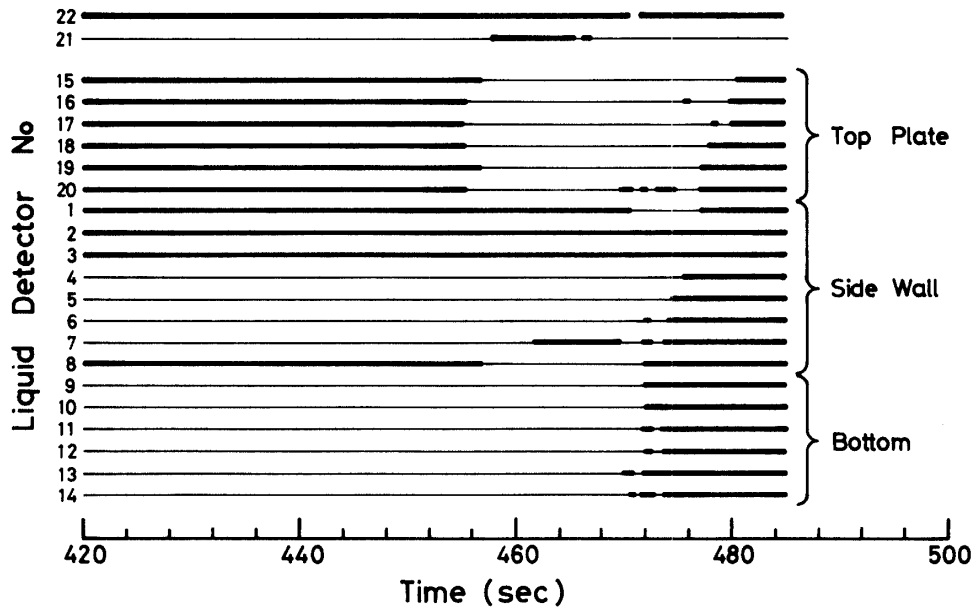

Fig. 11. c.

Fig. 11. Liquid detector results. Black circles and thick lines indicate liquid HeII state.
a. Initial stage of the flight; 0 through 65 sec.
b. Nearly Zero-g state; 200 through 280 sec.
c. Final stage of the flight; 420 through 485 sec. Effect of the reentry in the latter half.

cy was about 1.2 Hz around 60 sec, when the vehicle spin rate was about 0.5 Hz. This result seems to suggest that the rotating motion of HeII was rather close to a rigid body rotation in a breakdown state before the despin and that a considerable slip between the liquid and the vessel wall existed after the despin to result in a rapid damping of the rotating motion. The damping was as fast as in usual viscous fluids because the HeII was in a breakdown state. Actually, such motions were not detected after 95 sec. In addition

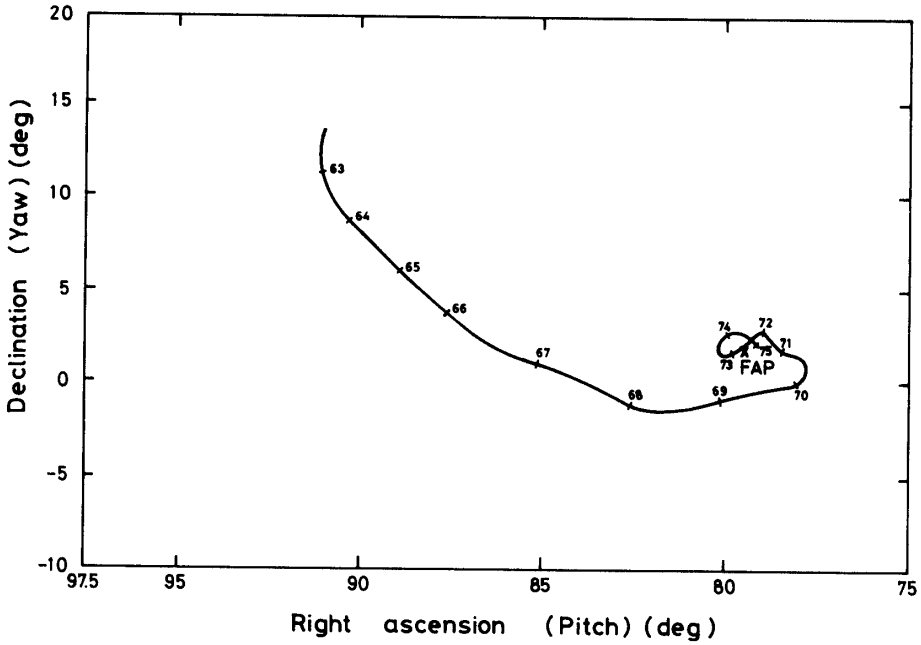

Fig. 12. a.

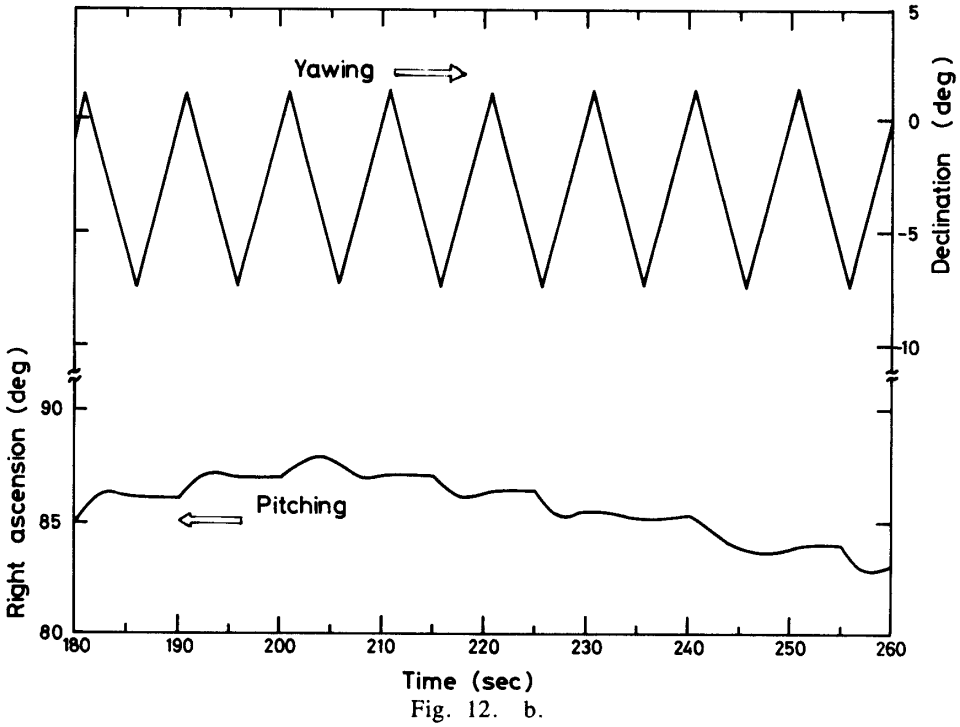

Fig. 12. b.

Fig. 12. Attitude of the payload section.

a. Transition motion to the first acquisition point FAP for raster scan. (Figures 63 through 75 indicate the time after the launch in sec)

b. Raster scan.

to these large scale motions, many small scale movements of the surface were recorded during this period. After 100 sec, both of the rotating motion in the tank resulting from spin and of moderately rapid motions also nearly damped, and a very slow but global HeII motion toward the top plate was observed around 150 sec.

The behavior of HeII was quite stable, and bulk HeII stayed on the top plate and at the two corners between the top plate and the side wall and between the bottom and the side wall after 200 sec. Only an appreciable HeII motion was periodical one detected by two detectors (10 and 11), of which the period was 10 sec as seen in Fig. 11-b. Such a periodical motion may be caused either by the liquid sloshing induced by the raster scan (Fig. 12-b), or by the persistent rotation of HeII under a subcritical condition. The critical velocity of the super component, v_{sc}, is supposed to be about 0.5 cm/s for this geometrical configuration. Thus, the period of the persistent rotation would be of the order of 100 sec which is much larger than the observation, and the amplitude of subcritical motion would be too small to be detected by the two detectors. The sloshing motion of HeII may be treated by the potential flow theory of capillary gravity waves [*10*], because peculiar behaviors of HeII must not appear in rather large scale motions under an isothermal situation. The natural angular velocity ω is given for capillary gravity waves by

$$\omega^2=\alpha k+\frac{\sigma}{\rho}k^3, \tag{1}$$

where ρ, σ and α are the density, the surface tension coefficient of HeII, and the acceleration, respectively, and k is the wave number which is estimated for the m-th mode to be

$$k=\frac{m\pi}{L} \tag{2}$$

in terms of the reference dimension L of the HeII tank. The first term of eq. (1) expresses the contribution from the acceleration, while the second from the surface tension. The frequency is written by

$$\nu=\omega/2\pi \tag{3}$$

These equations give an estimate of the natural sloshing frequency for the lowest mode to be about 0.1 Hz for $\alpha=10^{-3}$ g_0 and L=0.1 m. It is also seen from eq. (1) that both contributions from the acceleration and the surface tension are nearly comparable for such a situation. Now it comes to a conclusion that such periodical motion was induced by the raster scan, whose frequency was close to the resonance one of the sloshing motion of HeII in the HeII tank. Such a calm situation except for the scan induced motion persisted until about 450 sec.

The attitude variation caused by the out path scan starting at 402 sec and lasting for more than 40 sec was fairly fast, about 3 deg/sec, and large in magnitude, but no

appreciable HeII motions were detected as seen in Fig. 11-c. This indicates that the major part of liquid stayed in the top part of the tank and the induced acceleration by this scan motion pointed toward the bottom. Reentry caused violent large scale motions of the liquid after 455 sec. The axis of the payload section was close to horizontal at the beginning of the reentry, but the motion thereafter was supposed to be rather complex autorotation.

It is convenient to refer to the Bond number in order to investigate liquid motions in the low-gravity environment. This is defined by the ratio of the body force due to acceleration to the surface tension,

$$\mathrm{Bo}=\frac{\rho\alpha R_0^2}{\sigma}, \tag{4}$$

where R_0 is the radius of curvature of the free surface of bulk HeII. The Bond number diagram is given in Fig. 13 for HeII. For sufficiently small Bo, the surface tension dominates the liquid motion. Other rocket flight experiments had indicated that the threshold to the surface tension dominated situation was about 10^{-3} [*14*]. It seems that the result of the JPL onboard experiment [*5*], in which bulk HeII behavior was investigeated in a test cell partially filled with foam with pores 0.5 to 1 mm in diameter and with honeycomb with cells of 5 mm diameter, supports this conclusion. Thus, matrix structures with a reference length smaller than several mm can trap HeII as far as the acceleration is less than 10^{-3} g_0 as in the present case during the free fiight. In fact, HeII always stayed at the corners between the bottom and the side wall and between the top and the side wall, and the thermometer T_1 wrapped with fine woven copper wires whose pore size was far less than 1 mm was always in direct contact with HeII during this reduced gravity period.

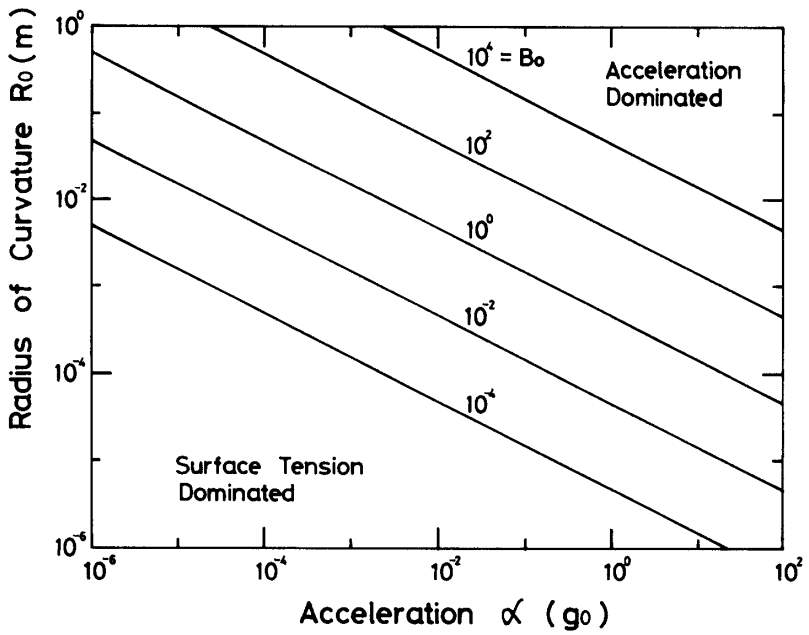

Fig. 13. Bond number diagram for HeII.

It can be now concluded that it took not a long time till the dynamic motion of HeII damped and that the situation was very stable and calm in both thermal and dynamical senses during the free flight. Also was a nearly isothermal state realized throughout the tank because of the wide extent of HeII distribution and/or thick adsorbed HeII film. It was also found that HeII remained in the tank in rather bulk state and located mostly at corners in the zero-gravity state.

(5) Film Flow Experiment

Thick (several hundreds Å) adsorbed film is formed on solid surfaces in the helium vapor environment below the lambda temperature, 2.172 K. In such film superfluid phenomena can happen. The thickness changes depending on the acceleration acting parallel to the film. It, in turn, quantitatively relates to the critical condition for superfluid breakdown. Thus, it is very important to investigate the effect of acceleration on the thickness for applications of the HeII cooling system in space.

This experiment was carried out by detecting the film breakdown in a heated pipe as illustrated in Fig. 14. In a circular pipe (oxygen-free copper, 10-mm-OD, 1-mm-thick and 165-mm-long), gaseous helium at 3 atm had been charged at the room temperature. One end (l_e=25 mm) was directly exposed to HeII working as a condenser, of which temperature was measured by a germanium resistance thermometer, T_1, and another had a manganin heater winding which supplied heat to an evaoprator (l_e=30 mm). The evaporator and the adiabatic section between the two sections were in the vacuum space located outside the HeII tank to ensure a perfect thermal isolation as illustrated in Fig.

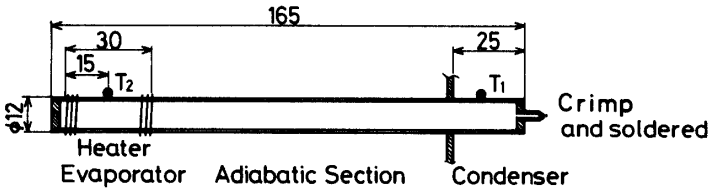

Fig. 14. Heat pipe for film flow experiment.

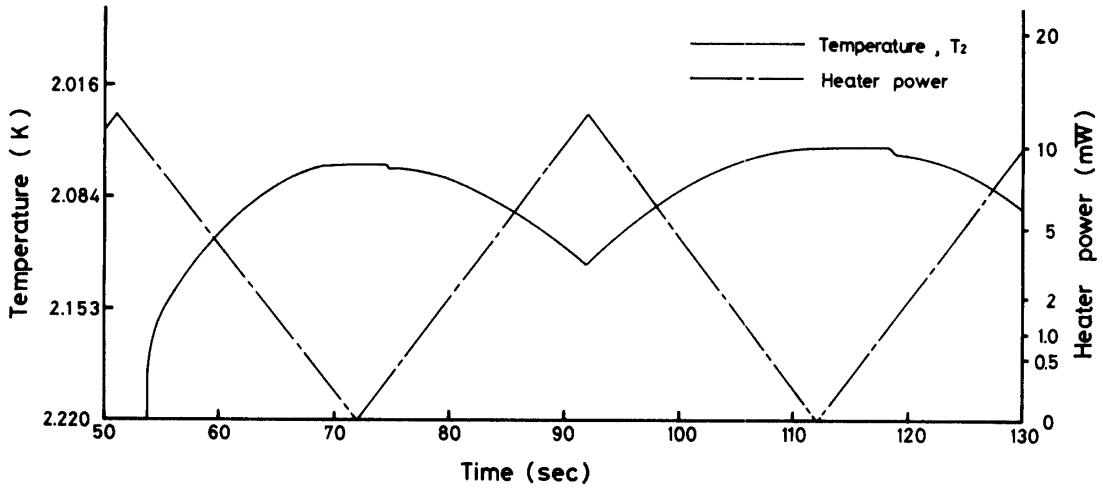

Fig. 15. Record of film flow experiment.

3-a. Linearly increasing and then decreasing current was supplied to the heater from 30 sec on. The period was 40 sec and the peak value was 17 mA (about 15 mW). The heat applied to the evaporator is transferred to the condenser through evaporating vapor, and the condensed vapor is returned to the evaporator in a form of thin film due to the thermomechanical effect. This may be considered as a simple superfluid heat pipe [*15*]. Superfluid breakdown can be detected as a sudden temperature rise, T_2, in the evaporator section.

A data record in the early part of the flight is given in Fig. 15. This shows that the superfluid breakdown state in the evaporator persisted until 54 sec, because of a rather high surrounding temperature T_6 as seen in Fig. 6 and the superfluid film suddenly recovered in the pipe to result in a temperature drop in T_2 at 54 sec. This is a result of superfluid film development. In the ground tests the breakdown state was observed while the pipe was set vertical with the evaporator top except at very low temperatures ($\leq$1.65 K). The recovery and breakdown were repeated nearly periodically responding to the periodical heating in the evaporator. It is seen in this particular example that the breakdown occurred at 74 sec and 118.5 sec. The temperature of the pipe soon become the same as that of HeII for the period of a subcritical heating condition, though it was higher than T_1 even for $Q=0$ in the early period shown in this figure. That is, it took about 100 sec to establish a quasi thermal equilibrium state.

This phenomenon can be treated quantitatively as follows. The heat input Q is related with the mass flow rate $\dot{M}$ in the form;

$$Q=\dot{M}(\lambda+TS), \tag{5}$$

where λ, S and T are the latent heat of vaporization, the specific entropy and the temperature, respectively. This expresses that a little part of heat is given to the super component flowing into the evaporator with zero-entropy and the rest evaporates the liquid helium. On the other hand, the thin film flow compensates the evaporated mass

$$\dot{M}=\rho_s D_w \delta V_s, \tag{6}$$

Here, D_w and δ are the wetted perimeter for film flow in the pipe and the film thickness, and ρ_s and V_s are the density and the velocity of the supper component in film, respectively. Eliminating $\dot{M}$ from eqs. (5) and (6), one obtaines the flow rate per unit length of the wetted perimeter

$$F=v_s\delta=\frac{Q}{\rho_s D_w(\lambda+TS)}. \tag{7}$$

The critical flow rate F_c can be obtained for the critical heat input Q_c, at which the superfluid breakdown occurs.

The theory of van der Waals adsorption suggests the thickness δ relates to the acceleration α and the height h above a liquid free surface as

$$\delta \propto (h\alpha)^{-1/3} \tag{8}$$

The proportional constant was experimentally found to be about 300 Å for $\alpha = 1.0\ g_0$ and h = 1 cm [*5*]. Therefore, film becomes thicker in reduced gravity conditions. In our experiment, a very large amount of helium was filled in the pipe, which corresponded to 8-μm-thick uniform film on the whole inside wall of the pipe. Very thick film, which may be considered as bulk HeII, would be formed in the pipe in the zero-gravity state, while the thickness had been controlled to be thinner than 400 Å by the use of a powder reservoir for helium in the JPL experiment [*5*].

Results are plotted in Fig. 16 together with two other data for comparison. One is a result obtained from experiments for the same pipe which was fixed horizontally in the one-g (ground) situation. Another is that for similar copper pipes which was fixed vertically with the evaporator above the condenser by 15 cm in the one-g condition. These data may be regarded as reflecting the effect of acceleration on the critical flow rate, primarily on the thickness. The F_c values for the zero-g and one-g horizontal are, indeed, larger than that for the one-g vertical, but not so large as the estimate by eq. (8), which predicts that the zero-g data should be more than 10 times of the one-g vertical data even at $\alpha = 10^{-3}\ g_0$. A uniform film thickness on the whole inner surface, 8 μm, as calculated from the helium inventory assuming that all helium participated in forming adsorption film, was not formed in the pipe. Major portion of HeII might be clamped in the corners at pipe ends because of surface tension, whose radius of curvature would be considerably small. It was also observed in the reentry stage of the flight that sudden breakdowns occurred even for a very small heating rate responding to variations of the acceleration resulting from the transition motion from the out path scan to the autorotation, and from the autorotation.

From a different point of view, this device may be regarded as a simple superfluid heat pipe [*15*], in which the heat transfer through evaporation and condensation and the

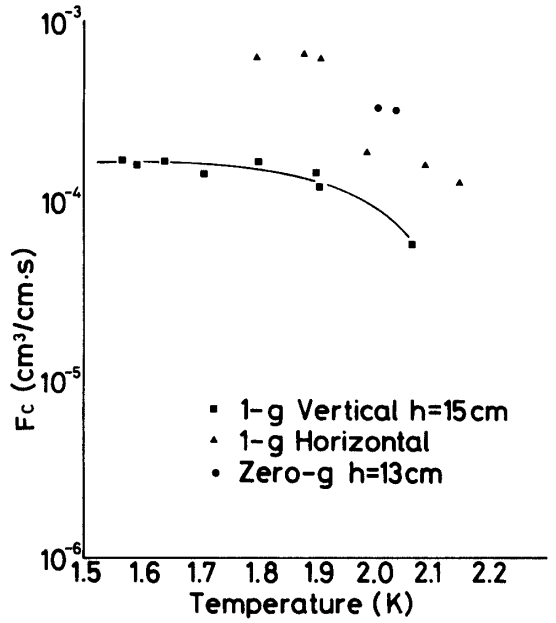

Fig. 16. Comparison of critical flow rates for film breakdown.

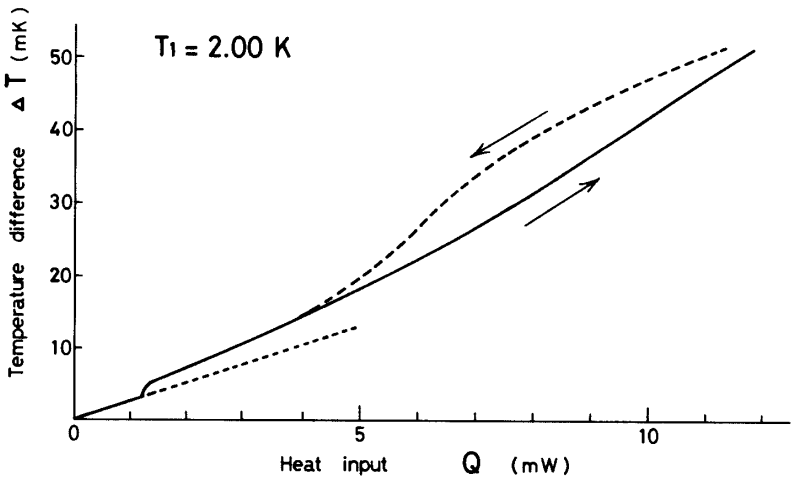

Fig. 17. Variation of temperature difference, $\Delta T=T_2-T_1$, with heat input Q.

passive liquid recirculation from the condenser to the evaporator due to the thermo-mechanical effect coexist. Excellent heat transport performance as well as the passive mechanism of liquid recirculation are the major features of the heat pipe. A typical example of the zero-g perforance for one heating cycle for 40 sec around 330 sec is shown in Fig. 17, in which the temperature difference $\Delta T(=T_2-T_1)$ between the evaporator and the condenser is plotted against the heat input Q to the evaporator. The condenser temperature T_1 was constant, 2.00 K, during this cycle. It is evident that the temperature of the evaporator T_2 slightly increased nearly linearly with Q for small Q and a temperature jump occurred at about 1.2 mW as the result of breakdown. The rate of the temperature rise with respect to Q became large under the supercritical heating condition. A hysteresis appeared only for higher Q as indicated by arrows in Fig. 17 because the increasing rate of Q was so rapid. However, it is evident that the critical value Q_C for the breakdown was free from the effect of hysteresis. The effective thermal conductivity κ_{eff} of the device is defined by

$$\kappa_{eff}=\frac{\ell_{HP}}{A_p}\frac{Q}{\Delta T}, \tag{9}$$

where ℓ_{HP} is given in terms of lengths of the evaporator ℓ_e, the condenser ℓ_c and the adiabatic section ℓ_{ad} by

$$\ell_{HP}=(\ell_e+\ell_c)/2+\ell_{ad}, \tag{10}$$

which was calculated to be 13.3 cm. The heat transfer area A_p is taken as the cross sectional one of the pipe, 0.79 cm^2. The values of $Q/\Delta T$ are obtained from Fig. 17 to be 0.42 W/K for the subcritical heating condition, and about 0.24 W/K for the supercritical one. The computed values of κ_{eff} are 6.4 W/K·cm for the subcritical and about 4 W/K·cm for the supercritical, respectively. These values are larger than the thermal conductivity of the pipe material (oxygen-free copper), 2 W/K·cm. It has to be borne in

mind that the experimental values are greatly degraded by the effect of Kapitza thermal resistance appearing at phase surfaces between HeII and solid participating in heat transfer such as at the evaporator and the condenser. Thus, detailed quantitative comparison of the values with those obtained in the Ref. 15 in the one-g state seems to be less meaningful. It should be concluded that the κ_{eff} value in the zero-g state was of the same order as that in the one-g state, though the former one is, in fact, larger than the latter by a factor of 2. On the other hand, the maximum heat transport capability, Q_{max}, which may be defined as the maximum of Q for which the superfluid heat pipe works with T_2 lower than thae lambda temperature, is considerably improved in the zero-g state because of the thick film.

(6) Cooled FET Pre-Amplifier Test

Noise generated by J-FET pre-amplifier for IR detectors (Infrared Lab. J-F230) was measured in the HeII temperature environment. The FET was installed on the outer wall of the top plate of the HeII tank as shown in Fig. 3-b, and was sensitive to mechanical vibrations because the element was suspended by fine threads to make sure of thermal isolation for thermal stabilization in the package. Microphonic noise caused by fluid induced vibrations would interfere signals from IR detectors. However, no such noise was detected during the free flight as seen in Fig. 18. In this figure only the ac components indicating the noise level are meaningfull. The Johnson noise level in this temperature range should be recorded as fluctuations in a couple of digits for $\Delta f=62$ Hz in this figure. Only appreciable noises beside the Johnson noise were genrated by mechanical shocks related with such rocket maneuvering motions as Yo-Yo-despinner development at 46 sec, nose cone ejection at 55 sec and the booster separtion at 60 sec. Even a large scale HeII motion, for example, the reversal of fluid location at 32 sec,

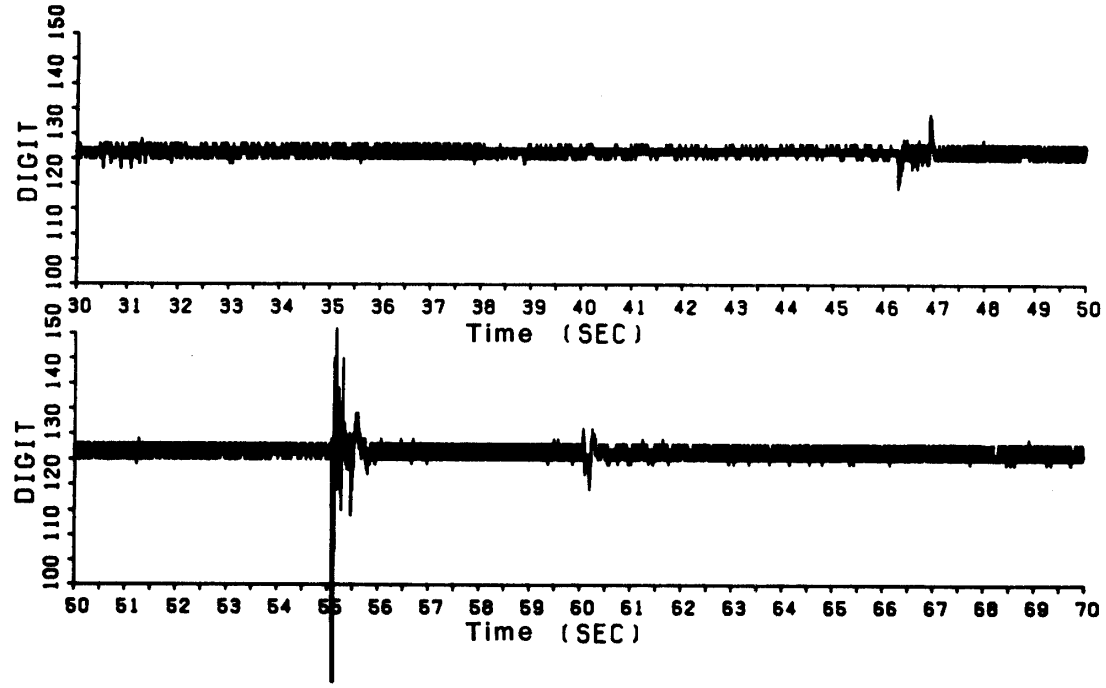

Fig. 18. J-FET pre-amplifier result. Only the ac components are shown. See the text for details.

produced negligibly small noise. It can be confirmed that this type of devices are of use for spaceborn cooled IR detection.

5. Conclusions

A superfluid cryostat was successfully flown aboard a sounding rocket for more than 8 min. The cryostate was of nearly realistic size for small scale space born cryogenic applications. All experiments could be conducted in a thermally stable situation and the following conclusions may be drawn.

i) The HeI remained stably in the tank and the temperature dropped very slowly, though the vapor exit was not equipped with a liquid-vapor phase separator.

ii) In the spin-dominant state, the HeII sat in a nearly rigid body rotation pressed against the side wall of the tank. This motion rapidly damped within not longer than 60 sec after the despin. This fact seems to indicate that the HeII was in the dynamically breakdown state during such spin-dominant period.

iii) The HeII distributed more or less uniformly in the tank, but the major portion held at the corners in the zero-g state.

iv) The temperature of the HeII was very stable and an isothermal state was realized in the tank throughout the zero-g period, when the maximum temperature difference was 15 mK even between the HeII and the outer wall of the tank. The temperature uniformity throughout the tank was far better than that in the one-g situation.

v) The porous-plug phase separator reached a steady state within 90 sec after the resumption of the vapor evacuation into space and worked perfectly both to perform a phase separation and to maintain the thermally stable environment in the tank.

vi) The dynamical behavior of the HeII was found to support an empirical criterion that the threshold value of the Bond number to the surface-tension-dominant situation was about 10^{-3}.

vii) The thickness of adsorbed film becomes thick in the zero-g state but is not so thick as estimate by the theory of van der Waals adsorption for thin film.

viii) The maximum heat transport capability, Q_{max}, of a superfluid heat pipe is improved in the zero-g state due to the growth of film thickness.

ix) The noise level caused by fluid induced vibrations in the tank was so low to be dtected by J-FET pre-amplifiers with a suspended structure in packages. This type of FET pre-amplifier may be compatible with the environment of space born IR telescopes.

Acknowledgement

The authers wish to express their appreciation to all the S520–3 staff for their cordial cooperation upon ground tests and launching operation. Particular thanks are extended to Mr. H. Koizumi for his contribution to onboard electronics package. The film flow experiment was supported in part by the Japan Radio Company (JRC).

REFERENCES

[1] Vorreiter, J. W., "Cryogenics for Spacecraft", Proc. of ICEC 7, 7th International Cryogenic Engineering Conference, 1978, pp. 1.
[2] van Duinen, R. J., "Infrared Astronomy", Proc. of ICEC 8, 1980, pp. 1.
[3] Mason, P. V., "Space Cryogenics in the 1980's", Proc. of ICEC 8, 1980, pp. 6.
[4] Mason, P., Collins, D., Petrac, D., Yang, L., Edeskuty, F. and Williamson, K., "Experiments on the Properties of Superfluid Helium in Zero Gravity", Proc. of ICEC 6, 1976, pp. 273.
[5] Mason, P., Collins, D., Petrac, D., Yang, L., Edeskuty, F., Schuch, A. and Willismson, K., "The Behavior of Sperfluid Helium in Zero Gravity", Proc. of ICEC 7, 1978, pp. 99.
[6] Petrac, D. and Mason, P., "Evaluation of Porous-Plug Liquid Separators for Space Superfluid Helium Systems", Proc. of ICEC 7, 1978, pp. 120.
[7] Yang, L. C. and Mason, P. V., "Superfluid helium film in zero gravity", Cryogenics, Vol. 20, No. 2, 1980, pp. 91.
[8] Murakami, M., Nakaniwa, N., Hayakawa, S., Matsumoto, T., Noguchi, K., Murakami, H., Uyama, K. and Nagano, H., "Superfluid Experiment in Zero Gravity aboard a Rocket", Proc. of ICEC 9, Kobe 1982, pp. 45.
[9] Hayakawa, S., Proc. Symp. on Advanced Instrumentation for Space Astronomy, Pergamon Press, 1982.
[10] Tanaka, W., Watanabe, T., Sawamura, M., Onaka, T., Yamaguchi, A., Nakagiri, M., Akita, K., Kodaira, K. and Nishi, K., "Spectroscopic Photometry in the Vacuum Ultra Violet of the Orion Region with the S-520-3-CN Rocket", ISAS Rept. SP-5, March 1983, pp. 35.
[11] Landau, L. D. and Lifshitz, E. M., Course of Theoretical Physics, Vol. 6, Fluid Mechanics. Addison-Wesley, 1959.
[12] Murakami, M., Nakaniwa, N., Nakai, H. and Uyama, K. "Vapor-Liquid Phase Separation of Superfluid HeII through Porous-Plug". to be published in ISAS Rept.
[13] Murakami, M., Nakaniwa, N., Uyama, K., "Porous Plug Phase Separator for Superfluid HeII", Proc. of ICEC 9, Kobe, 1982, pp. 194.
[14] Petrac, D., Gatewood, J. and Mason, P., "Sensor for Distinguishing Liqiud-Vapor Phases of Superfluid Helium", Advances in Cryogenic Engineering, Vol. 21, 1976, pp. 244.
[15] Murakami, M., Takeuchi, Y., Hayashi, T., Machida, T., Kato, S., Matsufuji, Y. and Hasui, T., "Thermal Behavior of Axially Grooved Heat Pipes aboard Rockets", ISAS Rept., No. 601, Institute of Space and Astronautical Science, 1982.
[16] Murakami, M., "Performance Investigation of Superfluid Heat Pipes", AIAA J. vol. 20, No. 4, 1982, pp. 570.